A WAVE PROPAGATION MATRIX METHOD IN SEMICLASSICAL THEORY

S.Y. LEE and N. TAKIGAWA
Institut de Physique Nucléaire
Division de Physique Théorique[+]
91406 Orsay Cedex - France

IPNO/TH 77-25 May 1977

[+]Laboratoire associé au C.N.R.S.

ABSTRACT

A wave propagation matrix method is used to derive the semiclassical formulae of the multi-turning point problem. A phase shift matrix and a barrier transformation matrix are introduced to describe the processes of a particle travelling through a potential well and crossing a potential barrier respectively. The wave propagation matrix is given by the products of phase shift matrices and barrier transformation matrices. We then apply the method to study scattering by surface transparent potentials and the Bloch wave in solids.

I. INTRODUCTION

Semiclassical approximation (or JWKB approximation) is of interest in many fields of physics. It often offers a clear physical picture of complicated processes and has been applied successfully in atomic molecular and nuclear physics etc. [1].

In our previous study [2, referred to as I]. We applied the semiclassical formula of the three turning point problem to study heavy ion optical potentials. In most cases agreement between quantal calculations and the semiclassical results were excellent. However the three turning-point formula failed to reproduce the Quantum mechanical S matrix of Gobbi's surface transparent potential [3] , where the imaginary potential has a smaller diffuseness and a smaller radius than those of the real potential. This potential has five important turning-points near to the real axis. This is because waves can be reflected not only by a real potential barrier but also by the surface of the imaginary potential. It is thus needed to extend the semiclassical theory to treat the problem with more turning points.

There exist many physical problems where one has to deal with more than three turning points. Fission through a double humped potential barrier and the Bloch wave in solids are two examples. A five turning point problem has been studied by Connor [4]. His method is, however, not easily generalizable.

In this study, we develop a semiclassical theory guided by a simple physical picture : When the particle travels through a region of no barrier, the wave function is multiplied by a phase shift matrix. When the particle crosses the barrier, the wave function is then multiplied by a barrier transformation matrix. This matrix method can easily be used to study complicated problems. In section 2, we rederive the semiclassical S matrix of the three turning point problem [5] by using the matrix method. In section 3, we give the barrier transformation matrix for the potential barrier which can be mapped onto a linear and a quatrutic functions. In section 4 we apply the method to study surface transparent potentials and to discuss the Bloch wave in solids. The conclusions are given in section 5.

II. DERIVATION OF THE SEMICLASSICAL S MATRIX

We reformulate the S matrix of the three turning point problem [5] , so that the method can easily be generalized. The problem is to solve the radial Schrödinger equation,

$$\frac{d^2\psi(r)}{dr^2} + \chi(r)\psi(r) = 0 \tag{1}$$

with

$$\chi(r) = \frac{2\mu}{\hbar^2}\,(E - V_\ell(r) - V_C(r) - V_N(r)) \tag{2}$$

where μ, E, $V_\ell(r)$, $V_C(r)$ and $V_N(r)$ are the reduced mass, the center of mass energy, the centrifugal potential, the Coulomb potential and the nuclear optical potential respectively. We assume that the effective potential $V(r) = V_\ell(r)+V_C(r)+V_N(r)$ is such that there are only three important turning points r_3, r_2 and r_1. r_3 is the most internal turning point, and r_2 and r_1 are turning points at the barrier (see Fig.1 of I).

We use the method of comparison functions [6]. In this method, we introduce an additional equation

$$\frac{d^2\varphi(\sigma)}{d\sigma^2} + \Gamma(\sigma)\varphi(\sigma) = 0 \tag{3}$$

such that $\Gamma(\sigma)$ is simple and Eq.(3) has well known exact solutions. Define the wave function $\psi_A(r)$ as

$$\psi_A(r) = \left(\frac{d\sigma}{dr}\right)^{-1/2}\varphi(\sigma) \tag{4}$$

The wave function $\Psi_A(r)$ is a good approximation to the solution of Eq.(1), provided that the mapping is chosen to be

$$\frac{d\sigma}{dr} = \left(\frac{\chi(r)}{\Gamma(\sigma)}\right)^{1/2} \tag{5}$$

and that the following condition is satisfied.

$$|\chi(r)| >> \frac{3}{4}\left(\frac{d\sigma}{dr}\right)^{-2}\left(\frac{d^2\sigma}{dr^2}\right)^2 - \frac{1}{2}\left(\frac{d\sigma}{dr}\right)^{-1}\frac{d^3\sigma}{dr^3} \tag{6}$$

Eq.(6) holds when the comparison function $\Gamma(\sigma)$ is very similar to $\chi(r)$ or when Planck's constant can be regarded as a small parameter [Ref.7,p.451]. To ensure the mapping is one to one and nonsingular, the zeros of $\chi(r)$, r_i, have to be mapped onto the zeros of $\Gamma(\sigma)$, σ_i. The branch cuts for $\chi^{1/2}$ and $\Gamma^{1/2}$ in r and σ spaces should be taken in a corresponding way. For the cut in r space, it is preferable that it does not cross the real axis. Eq.(5) implies that the semiclassical action integrals are identical in the two spaces.

$$\begin{aligned} S_i(r) &= S(r, r_i) \\ &= \int_{r_i}^{r} \sqrt{\chi}\, dr \\ &= \int_{\sigma_i}^{\sigma} \sqrt{\Gamma(\sigma')}\, d\sigma' \end{aligned} \tag{7}$$

The action integral from turning point r_i to r_j is denoted by S_{ij}.

To discuss the scattering for energies near the top of the barrier, we choose a quadratic and a linear comparison function in the barrier region (called region I) and in the interior region (called region II) respectively [5] , i.e.

$$\Gamma_{II}(\sigma) = (\sigma - \sigma_3) \tag{8}$$

$$\Gamma_{I}(\sigma) = \frac{\sigma^2}{4} - \epsilon \tag{9}$$

The mapping relation Eq.(7) gives that $\epsilon = -\frac{i}{\pi} S_{21}$.
The regular solution in region (II) is then

$$\Psi_{II}(r) = A_{II}\left(\frac{d\sigma}{dr}\right)^{-1/2} A_i(-(\sigma-\sigma_3)) \quad , \tag{10}$$

while the action integral $S_3(r)$ is given by

$$S_3(r) = \frac{2}{3}(\sigma - \sigma_3)^{3/2} \tag{11}$$

If σ is on the right hand side of σ_3 , we have $|\arg(\sigma-\sigma_3)| < \frac{2}{3}\pi$. Therefore if the action integral $S_3(r)$ is large, the wave function $\Psi_{II}(r)$ can well be approximated by its asymptotic form,

$$\Psi_{II}(r) \sim \frac{A_{II}}{2\sqrt{\pi}} (\chi(r))^{-1/4} [e^{i(S_3(r)-\pi/4)} + e^{-i(S_3(r)-\pi/4)}] \tag{12}$$

In Region (I), Eq.(3) has two linearly independent solutions, i.e. the Whittaker functions [7,8] , $D_{i\epsilon-1/2}(e^{i\pi/4}\sigma)$ and $D_{-i\epsilon-1/2}(e^{-i\pi/4}\sigma)$. The wave function can be expressed in terms of linear combinations of these Whittaker functions. The action

integral is

$$S(r) = \int_{\pm 2\sqrt{\epsilon}}^{\sigma} \left(\frac{\xi^2}{4} - \epsilon\right)^{1/2} d\xi$$

$$= \pm\left\{ \frac{\sigma^2}{4} - \frac{\epsilon}{2} + \frac{\epsilon}{2} \ell n\epsilon - \epsilon \ell n(\pm\sigma)\right\} \tag{13}$$

where the sign + or - should be taken according to whether σ is to the right hand side of $2\sqrt{\epsilon}$ or to the left hand side of $-2\sqrt{\epsilon}$. In arriving at Eq.(13), we have assumed explicitly that the branch cut in the ϵ plane is along the negative real axis. Let us define $\tilde{D}_{i\epsilon-1/2}(e^{i\pi/4}\sigma)$ and $\tilde{D}_{-i\epsilon-1/2}(e^{-i\pi/4}\sigma)$ as

$$\tilde{D}_{i\epsilon-1/2}(e^{i\pi/4}\sigma) \equiv e^{\frac{i3\pi}{8} - \frac{i}{2}\epsilon\ell n\epsilon/e + \pi\epsilon/4} D_{i\epsilon-1/2}(e^{i\pi/4}\sigma) \tag{14}$$

$$\tilde{D}_{-i\epsilon-1/2}(e^{-i\pi/4}\sigma) \equiv e^{\frac{-i3\pi}{8} + \frac{i}{2}\epsilon\ell n\epsilon/e + \pi\epsilon/4} D_{-i\epsilon-1/2}(e^{-i\pi/4}\sigma) \tag{15}$$

Then the incoming wave $\mathcal{J}(r)$ and outgoing wave $\mathcal{O}(r)$ solutions of Eq.(1) are given by

$$\mathcal{J}(r) \equiv \sqrt{2}\ \left(\frac{d\sigma}{dr}\right)^{-1/2} \tilde{D}_{i\epsilon-1/2}(e^{i\pi/4}\sigma)$$

$$\underset{r\to\infty}{\simeq} (\chi(r))^{-1/4}\ e^{-i(S_1(r)-\pi/4)} \tag{16}$$

$$\mathcal{O}(r) \equiv \sqrt{2}\ \left(\frac{d\sigma}{dr}\right)^{-1/2} \tilde{D}_{-i\epsilon-1/2}(e^{-i\pi/4}\sigma)$$

$$\underset{r\to\infty}{\simeq} (\chi(r))^{-1/4}\ e^{i(S_1(r)-\pi/4)} \tag{17}$$

where

$$S_l(r)-\pi/4 \underset{r\to\infty}{=} kr - \eta \ln 2kr - \frac{\pi}{2}(l+1) + \sigma_l + \delta_l \qquad (18)$$

We can write Eqs. (16) and (17) in a matrix form as

$$\begin{pmatrix} \mathcal{J}(r) \\ \mathcal{O}(r) \end{pmatrix} \underset{r\to\infty}{=} \begin{pmatrix} e^{-i\delta_l} & 0 \\ 0 & e^{i\delta_l} \end{pmatrix} \begin{pmatrix} \mathcal{J}_c(r) \\ \mathcal{O}_c(r) \end{pmatrix} \qquad (19)$$

where $\mathcal{J}_c(r)$, $\mathcal{O}_c(r)$ are the incoming and outgoing asymptotic scattering solutions of the Coulomb potential.

On the left hand side of the barrier, one can define the incoming wave $\Psi_-(r)$ and the outgoing wave $\Psi_+(r)$ as the waves moving towards the potential interior or out of the potential interior respectively. They can be expressed in the following matrix form

$$\begin{pmatrix} \Psi_-(r) \\ \Psi_+(r) \end{pmatrix} = \left(\frac{d\sigma}{dr}\right)^{-1/2} e^{\pi\varepsilon} \begin{pmatrix} N(i\varepsilon) & 1 \\ 1 & \bar{N}(i\varepsilon) \end{pmatrix} \begin{pmatrix} \tilde{D}_{i\varepsilon-1/2}(e^{i\pi/4}\sigma) \\ \tilde{D}_{-i\varepsilon-1/2}(e^{-i\pi/4}\sigma) \end{pmatrix}$$

$$\underset{r_3\ll r\ll r_2}{=} (\chi(r))^{-1/4} \begin{pmatrix} e^{-i(S_2(r)-\pi/4)} \\ e^{i(S_2(r)-\pi/4)} \end{pmatrix}, \qquad (20)$$

where $N(Z) = \dfrac{\sqrt{2\pi}}{\Gamma(\frac{1}{2}+Z)}\, e^{Z\ln Z/e}$ (21a)

and $\bar{N}(Z) = \dfrac{\sqrt{2\pi}}{\Gamma(\frac{1}{2}-Z)}\, e^{i\pi Z - Z\ln Z/e}$ (21b)

are the barrier penetration factors for the quadratic comparison function. Combined with Eqs.(16) and (17), Eq.(20) expresses the transformation of the incoming and the outgoing wave functions on the right hand side of the barrier into those on the left hand side of the barrier. The barrier transformation matrix B_Q is given by

$$B_Q = e^{\pi\varepsilon} \begin{pmatrix} N(i\varepsilon) & 1 \\ 1 & \bar{N}(i\varepsilon) \end{pmatrix} \tag{22}$$

The wave function in region I can be expressed as a linear combination of $\Psi_-(r)$ and $\Psi_+(r)$, i.e.

$$\begin{aligned} \Psi_I(r) &= A_I\, \Psi_-(r) + B_I\, \Psi_+(r) \\ &= (A_I, B_I) \begin{pmatrix} \Psi_-(r) \\ \Psi_+(r) \end{pmatrix} \end{aligned} \tag{23}$$

To match the wave function $\Psi_I(r)$ [Eq.(23)] with the wave function $\Psi_{II}(r)$ [Eq.(10)], we assume that there is a domain, where the asymptotic expressions Eqs.(12) and (20) are valid. Then the coefficients A_I and B_I are given by

$$\begin{pmatrix} A_I & 0 \\ 0 & B_I \end{pmatrix} = A_{II} \begin{pmatrix} e^{-iS_{32}} & 0 \\ 0 & e^{iS_{32}} \end{pmatrix} \tag{24}$$

This matrix, which we call as the phase shift matrix, expresses the phase shift of the wave travelling through the potential pocket. Thus from Eqs.(19),(20) and (24), the scattering wave function at large r can be written as

$$\psi(r) \underset{r\to\infty}{\simeq} A_{II}(1,1)\begin{pmatrix} e^{-iS_{32}} & 0 \\ 0 & e^{iS_{32}} \end{pmatrix}\begin{pmatrix} N(i\varepsilon) & 1 \\ 1 & \bar{N}(i\varepsilon) \end{pmatrix} e^{\pi\varepsilon}\begin{pmatrix} e^{-i\delta_1} & 0 \\ 0 & e^{i\delta_1} \end{pmatrix}\begin{pmatrix} \mathcal{J}_c(r) \\ \mathcal{O}_c(r) \end{pmatrix} \quad (25)$$

It would be worth pointing out that the matrix (1,1) is the boundary condition for a regular solution at the origin. Whereas the phase shift matrix and the barrier transformation matrix have nothing to do with the boundary condition, but depend solely on the properties of the potential well and the potential barrier.

In this derivation, one clearly sees the classical structure of the scattering problem, i.e., how a semiclassical particle picks up a phase shift, and how it crosses a potential barrier. Define the wave propagation matrix X as

$$\psi(r) \underset{r\to\infty}{\simeq} A_{II}(1,1)\begin{pmatrix} X_{11} & X_{12} \\ X_{21} & X_{22} \end{pmatrix}\begin{pmatrix} \mathcal{J}_c(r) \\ \mathcal{O}_c(r) \end{pmatrix} \quad (26)$$

The S matrix of the nuclear potential V_N is then given by

$$S = \frac{X_{12} + X_{22}}{X_{11} + X_{21}} \quad (27)$$

For the three turning point problem, one can show that

$$S = e^{2i\delta_1}\frac{1 + \bar{N}(i\varepsilon)e^{2iS_{32}}}{N(i\varepsilon) + e^{2iS_{32}}} \quad (28)$$

One can immediately apply this method to the problem of the double humpered barrier. Fig.1 shows schematically a

real double humped potential. When the energy is below the top of the barrier, there exist five turning points on the real axis as indicated in the figure. For a complex double humpered barrier, all of the turning points move into the complex r-plane, but the gross structure of the turning points does not change. We assume that the barriers (r_1,r_2) and (r_3,r_5) are far apart and that each can be approximated by a quadratic comparison function. The wave propagation matrix X is then given by

$$X = \begin{pmatrix} e^{-i\delta_{21}} & 0 \\ 0 & e^{i\delta_{21}} \end{pmatrix} \begin{pmatrix} N(i\delta) & i \\ i & \overline{N}(i\delta) \end{pmatrix} \begin{pmatrix} e^{-iS_{32}} & 0 \\ 0 & e^{iS_{32}} \end{pmatrix} \begin{pmatrix} N(i\delta) & i \\ i & \overline{N}(i\delta) \end{pmatrix} \begin{pmatrix} e^{-i\delta_{43}} & 0 \\ 0 & e^{i\delta_{43}} \end{pmatrix} e^{\pi\delta + \pi\varepsilon} \tag{29}$$

where $\varepsilon = -\frac{1}{\pi} S_{21}$ and $\delta = -\frac{1}{\pi} S_{53}$ are action integrals of the barriers (r_2,r_1) and (r_5,r_3) respectively. The S matrix becomes

$$S = \frac{e^{2i\delta_1}}{N(i\delta)} + \frac{e^{2i\delta_1}}{N(i\delta)} e^{iS_{21}} \left\{ \frac{e^{iS_{32}}}{N(i\delta)N(i\delta)} + \frac{e^{iS_{42}}}{N(i\delta)N(i\delta)} \frac{1}{1 + \frac{e^{iS_{43}}}{N(i\delta)}} \right\} \Bigg/$$

$$\Bigg/ \left\{ 1 + \frac{e^{iS_{32}}}{N(i\delta)N(i\delta)} + \frac{e^{iS_{42}}}{N(i\delta)N(i\delta)} \frac{1}{1 + \frac{e^{iS_{43}}}{N(i\delta)}} \right\} \tag{30}$$

The physics of Eq.(30) is clear. The first term describes the wave reflection at the most external turning point r_1. The internal waves reflected from turning points r_3 and r_4 interfere. They are also modified by multiple reflections. Notice that there exist multiple reflections between r_3 and r_2 , r_4 and r_2 and also between r_4 and r_5.

The above example of a five turning point problem shows clearly the flexibility of the method. The matrix products cook the "quantum soup" with the "classical bones". In the next section, we discuss the barrier transformation matrices for linear and quadratic barriers.

III. THE BARRIER TRANSFORMATION MATRIX (B)

To ensure a good approximation, the comparison function $\Gamma(\sigma)$ must simulate the topological structure of $\chi(r)$ well. Hence $\Gamma(\sigma)$ has to be chosen carefully according to various physical situations. In this section, we derive the barrier transformation matrices which correspond to linear and quadratic comparison functions. They are commonly used to deal with physical problems. This is because the solutions of the comparison equation are well known and simple. The barrier transformation matrices can then be obtained by studying the asymptotic behaviour of the Airy and the Whittaker functions respectively. The normalization of the wave functions implies that the determinant of the barrier transformation matrix is equal to 1.

III.1. The quadratic comparison function : $\Gamma(\sigma) = (\frac{\sigma^2}{4} - \varepsilon)$

A one to one mapping of $r \leftrightarrow \sigma$ spaces implies that $\varepsilon = -\frac{1}{\pi} S_{ab}$, where r_a and r_b are two turning points of the barrier. The equipotential contour of $\Gamma(\sigma)$ in the $\sigma = \sigma_R + i\,\sigma_I$ plane can be visualized through

$$\mathrm{Re}\Gamma(\sigma) = \frac{\sigma_R^2 - \sigma_I^2}{4} - \varepsilon_R \qquad (31)$$

$$\mathrm{Im}\Gamma(\sigma) = \frac{1}{2}\,\sigma_R\sigma_I - \varepsilon_I \qquad (32)$$

Along the real and imaginary σ axes, $\mathrm{Re}\Gamma(\sigma)$ is a quadratic function, while $\mathrm{Im}\Gamma(\sigma)$ is a linear function. Thus, if the real part of the potential energy surface along the real axis looks like a parabola, it would be reasonable to use the quadratic comparison function.

On the other hand, if we have a potential barrier of Woods-Saxon type,

$$V(Z) = \frac{V_0}{(1+ e^{(Z-R)/a})} , \tag{33}$$

we have one real turning point when the energy E is below the barrier height V_0. It is reasonable to use the linear comparison function $\Gamma(\sigma) = \sigma-\sigma_0$. Whereas, when the energy E is well above the barrier V_0, we have two turning points Z_0 and Z_0^* near the real axis. In this case, the energy surface looks linear along the real axis and quadratic along the line connecting Z_0 and Z_0^*, i.e.

$$\chi(Z) \underset{\text{along } Z, Z_0^*}{\sim} (Z-Z_0)(Z-Z_0^*) . \tag{34}$$

If both turning points Z_0 and Z_0^* are important in the problem, we may use the parabolic comparison function between Z_0 and Z_0^*. In most practical applications, however, only one of the turning points is important. This is because the action integral between Z_0 and Z_0^* is large so that the effect of the barrier penetration factor is not important. The S matrix of the quadratic comparison function reduces to a single turning point formula with a linear comparison function (see section IV.1).

The derivation of the preceeding section gives the barrier transformation matrix of the quadratic barrier,

$$B_Q = e^{\pi\varepsilon} \begin{pmatrix} N(i\varepsilon) & 1 \\ 1 & \bar{N}(i\varepsilon) \end{pmatrix} \tag{35}$$

The wave functions to the left hand side of the barrier $\phi^L(r)$ and to the right hand side $\phi^R(r)$ are related by

$$\begin{pmatrix} \phi_-^L(r) \\ \phi_+^L(r) \end{pmatrix} = B_Q \begin{pmatrix} \phi_-^R(r) \\ \phi_+^R(r) \end{pmatrix} \tag{36}$$

where

$$\phi_\mp^L(r) \sim (\chi(r))^{-1/4} e^{\mp i(S_{r_L}(r)-\pi/4)} \tag{37}$$

and r_L is the turning point to the left hand side of the barrier. Eq.(37) indicates that $\phi_-(r)$ and $\phi_+(r)$ describe the wave propagating to the left and to the right respectively. The inverse of Eq.(36) leads to

$$\begin{pmatrix} \phi_-^R(r) \\ \phi_+^R(r) \end{pmatrix} = B_Q^{-1} \begin{pmatrix} \phi_-^L(r) \\ \phi_+^L(r) \end{pmatrix}$$

where

$$B_Q^{-1} = e^{\pi\varepsilon} \begin{pmatrix} \bar{N}(i\varepsilon) & -1 \\ -1 & N(i\varepsilon) \end{pmatrix} \tag{39}$$

III.2. The linear comparison function $\Gamma(\sigma) = c(\sigma-\sigma_0)$

The linear comparison function is the most commonly used mapping function for the derivation of semiclassical connection formula. The solution of Eq.(3) is then the regular and the irregular Airy functions $Ai(-c^{1/3}(\sigma-\sigma_0))$ and $Bi(-c^{1/3}(\sigma-\sigma_0))$. The condition given by Eq.(5) implies that the action integral $S_0(r)$ is given by

$$\begin{aligned} S_0(r) &= \int_{r_0}^{r} \sqrt{\chi(r')}dr' \\ &= \int_{\sigma_0}^{\sigma} \sqrt{c(\sigma'-\sigma_0)}d\sigma' \\ &= c^{1/2}\,\frac{2}{3}(\sigma-\sigma_0)^{3/2} \end{aligned} \tag{40}$$

There exist also other sets of linearly independent solutions, e.g. $Ai(-e^{i2\pi/3}c^{1/3}(\sigma-\sigma_0))$, $Ai(-e^{-i2\pi/3}c^{1/3}(\sigma-\sigma_0))$ etc.. We can always choose a convenient set of independent solutions to work out the barrier transformation matrix. The barrier transformation matrix depends on the cut in the r and/or σ planes. This is because the interpretation of a wave propagating to the left side or to the right side of a barrier depends on the cut.

Let us consider at first the problem of a real potential with a real turning point r_0. We list below the transformation of the wave function for $c = -1$ and/or $c = +1$ from one side on the real axis to the other side on the real axis. $c = -1$ and $c = 1$ correspond to the cases where the classically forbidden region is to the right and to the left of σ_0 respectively.

I. $\gamma(\sigma) = -(\sigma - \sigma_0)$

$$\begin{pmatrix} \Phi_-^{\downarrow}(r) \\ \Phi_+^{\uparrow}(r) \end{pmatrix} \leftrightarrow \begin{pmatrix} 1/2 & 1 \\ -1/2 & 1 \end{pmatrix} \begin{pmatrix} \Phi_-^{\uparrow}(r) \\ \Phi_+^{\downarrow}(r) \end{pmatrix} \tag{41a}$$

$$\begin{pmatrix} \Phi_-^{\uparrow}(r) \\ \Phi_+^{\downarrow}(r) \end{pmatrix} \leftrightarrow \begin{pmatrix} 1 & -1/2 \\ 1 & 1/2 \end{pmatrix} \begin{pmatrix} \Phi_-^{\downarrow}(r) \\ \Phi_+^{\uparrow}(r) \end{pmatrix} \tag{41b}$$

$$\begin{pmatrix} \Phi_-^{\uparrow}(r) \\ \Phi_+^{\downarrow}(r) \end{pmatrix} \leftrightarrow \begin{pmatrix} 1 & 1 \\ 0 & 1 \end{pmatrix} \begin{pmatrix} \Phi_-^{\downarrow}(r) \\ \Phi_+^{\uparrow}(r) \end{pmatrix} \tag{42a}$$

$$\begin{pmatrix} \Phi_-^{\downarrow}(r) \\ \Phi_+^{\uparrow}(r) \end{pmatrix} \leftrightarrow \begin{pmatrix} 1 & 0 \\ 1 & 1 \end{pmatrix} \begin{pmatrix} \Phi_-^{\uparrow}(r) \\ \Phi_+^{\downarrow}(r) \end{pmatrix} \tag{42b}$$

where $\Phi_\pm(r) \sim \chi^{-\frac{1}{4}} e^{\pm i[S_{r_0}(r) - \frac{\pi}{4}]}$.

II. $\Gamma(\sigma) = (\sigma - \sigma_0)$

$$\begin{pmatrix} \Phi_-^{\uparrow}(r) \\ \Phi_+^{\downarrow}(r) \end{pmatrix} \leftrightarrow \begin{pmatrix} 1/2 & -1/2 \\ 1 & 1 \end{pmatrix} \begin{pmatrix} \Phi_-^{\downarrow}(r) \\ \Phi_+^{\uparrow}(r) \end{pmatrix} \tag{43a}$$

$$\begin{pmatrix} \Phi_-^{\downarrow}(r) \\ \Phi_+^{\uparrow}(r) \end{pmatrix} \leftrightarrow \begin{pmatrix} 1 & 1 \\ -1/2 & 1/2 \end{pmatrix} \begin{pmatrix} \Phi_-^{\uparrow}(r) \\ \Phi_+^{\downarrow}(r) \end{pmatrix} \tag{43b}$$

$$\begin{pmatrix} \Phi_-^{\uparrow}(r) \\ \Phi_+^{\downarrow}(r) \end{pmatrix} \leftrightarrow \begin{pmatrix} 1 & 0 \\ 1 & 1 \end{pmatrix} \begin{pmatrix} \Phi_-^{\downarrow}(r) \\ \Phi_+^{\uparrow}(r) \end{pmatrix} \tag{44a}$$

$$\begin{pmatrix} \Phi_-^{\downarrow}(r) \\ \Phi_+^{\uparrow}(r) \end{pmatrix} \leftrightarrow \begin{pmatrix} 1 & 1 \\ 0 & 1 \end{pmatrix} \begin{pmatrix} \Phi_-^{\uparrow}(r) \\ \Phi_+^{\downarrow}(r) \end{pmatrix} \tag{44b}$$

The symbols $\uparrow$ and $\downarrow$ indicate the exponential increase or decrease of the wave function as r goes away from the turning point r_0. The (2×2) matrices in Eqs.(41) through (44) define the barrier transformation matrices.

When the particle travels through two linear barriers, any pair of matrices in Eqs.(41) and (43) or Eqs.(42) and (44) can be chosen to construct the wave propagation matrix. A convenient choice is such that the corresponding phase shift matrix between two turning points becomes diagonal. Then the barrier transformation matrix should be taken pairwise, such as Eqs.(41a) with (43a), Eqs.(41b) with (43b), Eqs.(42a) with (44a) or Eqs.(42b) with (44b).

These transformation matrices are practically equivalent in all physical problems. Eqs.(41) and (43) are, however, preferred for real potentials with real turning points, because the final semiclassical S matrix is unitary. This argument is equivalent to the reality condition of the wave function in the classically allowed region [9]. Eqs.(42) and (44) do not give a unitary S matrix, but the large component of the wave function agrees with that of Eqs.(41) and (43). We give the following example to demonstrate the use of the above transformation matrices. Consider a particle tunneling through a potential barrier formed by two linear barriers on both ends. The wave functions to the left hand side of the barrier is connected to that to the right hand side of the barrier by

$$\begin{pmatrix} \Phi_-^L(r) \\ \Phi_+^L(r) \end{pmatrix} \leftrightarrow \begin{pmatrix} \frac{1}{2} & 1 \\ -\frac{1}{2} & 1 \end{pmatrix} \begin{pmatrix} e^{-\pi\varepsilon} & 0 \\ 0 & e^{\pi\varepsilon} \end{pmatrix} \begin{pmatrix} \frac{1}{2} & -\frac{1}{2} \\ 1 & 1 \end{pmatrix} \begin{pmatrix} \Phi_-^R(r) \\ \Phi_+^R(r) \end{pmatrix}$$

$$= \begin{pmatrix} e^{\pi\varepsilon}(1+\frac{1}{2}e^{-2\pi\varepsilon}) & e^{\pi\varepsilon}(1-\frac{1}{2}e^{-2\pi\varepsilon}) \\ e^{\pi\varepsilon}(1-\frac{1}{2}e^{-2\pi\varepsilon}) & e^{\pi\varepsilon}(1+\frac{1}{2}e^{-2\pi\varepsilon}) \end{pmatrix} \begin{pmatrix} \Phi_-^R(r) \\ \Phi_+^R(r) \end{pmatrix} \qquad (45)$$

or

$$\begin{pmatrix} \Phi_-^L(r) \\ \Phi_+^L(r) \end{pmatrix} \leftrightarrow \begin{pmatrix} 1 & 1 \\ 0 & 1 \end{pmatrix} \begin{pmatrix} e^{-\pi\varepsilon} & 0 \\ 0 & e^{\pi\varepsilon} \end{pmatrix} \begin{pmatrix} 1 & 0 \\ 1 & 1 \end{pmatrix} \begin{pmatrix} \Phi_-^R(r) \\ \Phi_+^R(r) \end{pmatrix}$$

$$= \begin{pmatrix} e^{\pi\varepsilon}(1+e^{-2\pi\varepsilon}) & e^{\pi\varepsilon} \\ e^{\pi\varepsilon} & e^{\pi\varepsilon} \end{pmatrix} \begin{pmatrix} \Phi_-^R(r) \\ \Phi_+^R(r) \end{pmatrix} \qquad (46)$$

where $\varepsilon = -\frac{i}{\pi} S_{21}$. On the other hand, for energies far below a quadratic barrier, Eq.(22) gives the following barrier transformation matrix,

$$B_Q = \begin{pmatrix} e^{\pi\varepsilon}(1+e^{-2\pi\varepsilon})^{1/2} & e^{\pi\varepsilon} \\ e^{\pi\varepsilon} & e^{\pi\varepsilon}(1+e^{-2\pi\varepsilon})^{1/2} \end{pmatrix} \qquad (47)$$

This is very similar to Eqs.(45) and (46). Eqs.(45), (46) and (47) are actually equivalent in many applications, since they have the same large component of the wave function in the classically forbidden region.

In the case of an imaginary potential barrier, there are in general two turning points near the real axis (see Appendix). Near the turning points, the energy surface is a monotonic function along the real axis. As we have noted in the previous section, it looks like a quadratic function between the two turning points. Here we will study the linear mapping function $\Gamma(\sigma)=\pm i(\sigma-\sigma_0)$,

where σ_0 is not a real number. The cut in the σ plane is chosen in such a way that it does not cross the real axis. From this we obtain the following connection formulae ;

$$\Gamma(\sigma) = \pm i(\sigma-\sigma_0)$$

(a) when σ_0 is in the lower σ plane,

$$\begin{pmatrix} \phi_-^L(r) \\ \phi_+^L(r) \end{pmatrix} \rightarrow \begin{pmatrix} 1 & 1 \\ 0 & 1 \end{pmatrix} \begin{pmatrix} \phi_-^R(r) \\ \phi_+^R(r) \end{pmatrix} \tag{48}$$

(b) when σ_0 is in the upper σ plane,

$$\begin{pmatrix} \phi_-^L(r) \\ \phi_+^L(r) \end{pmatrix} \rightarrow \begin{pmatrix} 1 & 0 \\ 1 & 1 \end{pmatrix} \begin{pmatrix} \phi_-^R(r) \\ \phi_+^R(r) \end{pmatrix} \tag{49}$$

where $\phi^L(r)$ and $\phi^R(r)$ are the wave functions to the left hand side and to the right hand side of the barrier. The above formulae are generally valid for regions nearest to the real axis. There exist other linear barrier transformation matrices which are valid in other domains of the space.

One observes from Eqs.(48) and (49) that if the turning point is in the lower σ or r plane, there is no reflection for the wave coming from the left side of the barrier, i.e. $\phi_+^L = \phi_+^R$. Whereas if the turning point is above the real axis, there is no reflection for the wave coming from the right, i.e. $\phi_-^R = \phi_-^L$. This implies that the position of the turning point is much more important than the structure of the Stokes lines for determining the physical process. The structure of the

linear transformation matrix enables us to understand the structure of turning points and their Stokes lines studied in Ref. 10 . For example, with the notation of Ref.10, the process (1,2),3) is related to Eq.(49) by

$$\Psi(r) \underset{r\to\infty}{\simeq} A(t,\bar{t}) \begin{pmatrix} e^{-iS_{21}} & 0 \\ 0 & e^{iS_{21}} \end{pmatrix} \begin{pmatrix} 1 & 0 \\ 1 & 1 \end{pmatrix} \begin{pmatrix} e^{-iS_{11}} & 0 \\ 0 & e^{iS_{11}} \end{pmatrix} \begin{pmatrix} 1 & 0 \\ 1 & 1 \end{pmatrix} \begin{pmatrix} e^{-i\delta_1} & 0 \\ 0 & e^{i\delta_1} \end{pmatrix} \begin{pmatrix} \phi_t^{(1)} \\ \phi_t^{(2)} \end{pmatrix} \tag{50}$$

All other processes in Ref.10 can be understood in terms of the matrices of this section.

IV. APPLICATIONS

IV.1. Scattering from Surface Transparent Potentials

Surface transparent potentials are often used to analyze light heavy ion elastic scattering. We will consider $^{18}O - ^{16}O$ scattering at $E_{cm} = 20$ MeV by the following potential,

$$V(r) = - \frac{V_0}{1 + e^{(r-R_0)/a_0}} - i \frac{W_0}{1 + e^{(r-R_W)/a_W}} \qquad (51)$$

with $(V_0 , R_0 , a_0) = (17 \text{ MeV}, 6.8 \text{ fm}, 0.49 \text{ fm})$

$(W_0 , R_W , a_W) = (4.8 \text{ MeV}, 6.4 \text{ fm}, 0.30 \text{ fm})$

The imaginary part of this potential has a smaller radius and diffuseness than the real part. The turning points are presented in Fig.2, where we observe that there are five turning points near the real axis for each partial wave. The external turning points r_1 and r_2 are due to the potential barrier of the Coulomb, the centrifugal and the attractive nuclear potentials. The potential energy surface near r_1 and r_2 looks parabolic. The most internal turning point r_4 is also essentially due to the centrifugal and the strong attractive nuclear potentials. The real part of the potential energy surface near this turning point can be simulated by a linear comparison function. The remaining two turning points r_5 and r_3 are probably due to the change of the energy surface of the imaginary potential [see Appendix].

The energy surface is monotonic along the real axis, but is rather complicated along the line joining two turning points r_5 and r_3 . However, the detail properties of the barrier around (r_5, r_3) are not important, because the action integral S_{53} is large. The wave function prefers propagating along the real axis. This is equivalent to setting

$$N(i\delta) = 1$$

in Eq.(30), where we have assumed explicitly a parabolic barrier for (r_5, r_3). Furthermore, since the turning points r_4 and r_5 are far away from the real axis, multiple reflections are not important. Eq.(30) thus reduces to

$$S = \frac{e^{2i\delta_1}}{N(i\varepsilon)} + \frac{e^{2i\delta_1}}{N(i\varepsilon)} e^{2iS_{21}} \left(\frac{e^{2iS_{32}}}{N(i\varepsilon)} + \frac{e^{2iS_{42}}}{N(i\varepsilon)} \right) \frac{1}{1 + \frac{e^{2iS_{32}}}{N(i\varepsilon)} + \frac{e^{2iS_{42}}}{N(i\varepsilon)}} \quad (52)$$

Eq.(52) can also be derived by assuming a linear comparison function $\Gamma(\sigma) = -i(\sigma - \sigma_3)$ for the turning points r_3. The wave propagation matrix can be written as

$$X = \begin{pmatrix} e^{-iS_{43}} & 0 \\ 0 & e^{iS_{43}} \end{pmatrix} \begin{pmatrix} 1 & 1 \\ 0 & 1 \end{pmatrix} \begin{pmatrix} e^{-iS_{32}} & 0 \\ 0 & e^{iS_{32}} \end{pmatrix} \begin{pmatrix} N & 1 \\ 1 & \bar{N} \end{pmatrix} e^{\pi\varepsilon} \begin{pmatrix} e^{-i\delta_1} & 0 \\ 0 & e^{i\delta_1} \end{pmatrix} \quad (53)$$

It is easy to prove that Eq.(53) gives the same S matrix as Eq.(52). The physical meaning of each term in Eq.(53) is also clear from the discussion of section II.

The results of the calculation are shown in Figs.3 and 4. The semiclassical internal wave S matrix [second term of Eq.(52)] is compared with the quantum mechanical internal

wave S matrix η_I^Q, which is defined as the difference between the S matrix of the quantum mechanical calculation and the semiclassical barrier wave S matrix η_B [first term of Eq.(52)]. The imaginary potential in this calculation is relatively strong, so that the multiple-reflections in Eq.(52) is not important. The internal waves reflected from turning points r_3 and r_4 interference with each other. This interference gives rise to a complicated structure in the internal wave S matrix. The Argand diagram of the internal wave S matrix seems to indicate that interference of internal waves simulates the phase shift of a deep real potential . The interference also gives rise to oscillations in the amplitude of the internal wave S matrix (Fig.5). This behaviour of the internal wave S matrix is very different from that studied in I. It would be worthwhile to point out that the internal wave S matrix is not sharply peaked at the surface partial waves. The main characteristics of this potential is not the surface transparency, but the interference of the internal waves. This contrasts to the case of McVoy's surface transparent potential [see I].

Gobbi et al. have analyzed the $^{16}O - ^{16}O$ scattering with a surface transparent potential, where the parameter α_w in Eq.(51) is 0.15 fm [3] . The structure of the turning points (Fig.6) is very similar to that of Fig.2. Turning points r_5 and r_3 are nearer to the real axis in this case. However, the action integral S_{53} is still large. Hence the S matrix of the five turning point problem [Eq.(30)] reduces to that of the four turning point problem [Eq.(52)].

Fig.7 compares the amplitude of the semiclassical internal wave S matrix with the amplitude of quantum mechanical

internal wave S matrix. The amplitude o the semiclassical S matrix is much larger. This discrepancy is probably due to the fact that the strength of the imaginary potential $\sqrt{\mu W_n a_w^2}$ is very small and the wave length is longer than the diffuseness of the imaginary potential. As is known, the reflection coefficient of a semiclassical wave from such a barrier becomes much larger than the exact quantum mechanical value [11]. However the phase relation between the two semiclassical internal waves seems correct and gives rise to an interference pattern which is very similar to that of the quantum mechanical internal wave S matrix. Although the semiclassical calculation fails to reproduce the magnitude of the internal wave S matrix given by the quantum mechanical calculation, the conclusion we had for the case of a = 0.30 fm should also be applicable to understand the characteristic features of this potential.

To emphasize the conclusion again : The surface transparent potential of Gobbi et al is transparent not only for surface partial waves but for all partial waves. The internal wave reflected from the imaginary potential barrier interferes with that reflected from the most inner barrier formed essentially by real potentials. Because of the interference, the internal wave amplitude peaked at some partial waves and the phase shift of the total internal wave resembles that of a deep real potential.

Pokrovskii and Khalatnikov [12] have extended the semiclassical theory to take into account the pole and the zero of $\chi(r)$. This generalization could resolve the difficulty of JWKB theory at high energies with a shallow potential, where the zero and the pole lie very near to each other.

IV.2 The Bloch wave

We apply the method of a wave propagation matrix to the problem of electrons in solids. The electron experiences potential barriers near the lattice sites. We assume that the one dimensional periodic potential barrier can be mapped onto a parabolic form. The stationary state solution implies that the wave function is periodic in its modulus. i.e.

$$\Psi(x + d) = \alpha\, \Psi(x) \qquad \text{with } |\alpha| = 1 \quad , \tag{54}$$

where d is the size of the lattice. Using the wave propagation matrices, the wave function can be expressed as

$$\Psi_m(x) = (c_1, c_2)\left[\begin{pmatrix} e^{-iS} & 0 \\ 0 & e^{iS} \end{pmatrix} e^{\pi\varepsilon}\begin{pmatrix} N(i\varepsilon) & 1 \\ 1 & \bar{N}(i\varepsilon) \end{pmatrix}\right]^m \begin{pmatrix} \phi_-(x) \\ \phi_+(x) \end{pmatrix} \tag{55}$$

where S is the action integral of the potential well, and $i\pi\varepsilon$ is the action integral of the barrier. The periodicity condition [Eq. (54)] implies that

$$\det \begin{bmatrix} e^{\pi\varepsilon} N(i\varepsilon) e^{-iS} - \alpha & , & e^{\pi\varepsilon}\, e^{-iS} \\ e^{\pi\varepsilon} \quad e^{iS} & , & e^{\pi\varepsilon} \bar{N}(i\varepsilon) e^{iS} - \alpha \end{bmatrix} = 0 \tag{56}$$

i.e.

$$\alpha^2 - e^{\pi\varepsilon}\,(N e^{-is} + \bar{N} e^{is})\,\alpha + 1 = 0$$

$$\alpha^2 - e^{\pi\varepsilon}(N\, e^{-is} + \bar{N}\, e^{is})\alpha + 1 = 0$$

Defining $N = a\, e^{i\varphi}$, we have

$$\bar{N} = \begin{cases} a\, e^{-i\varphi} & \text{, for energy below the barrier } E < V_B \\ e^{-2\pi\varepsilon} a\, e^{-i\varphi} & \text{, for energy above the barrier } E > V_B \end{cases}$$

Eq. (56) then becomes

$$\begin{cases} \alpha^2 - 2\,\dfrac{a}{\sqrt{a^2-1}}\cos(S-\varphi)\cdot\alpha+1 = 0 & (\text{for } E\lesssim V_B) \qquad (57a) \\ \alpha^2 - 2a\cos(\mathrm{Re}S-\varphi)\alpha+1 = 0 & (\text{for } E>V_B)\ , \qquad (57b) \end{cases}$$

where ReS is the real part of S. The solutions of Eqs. (57a) and (57b) are respectively.

$$\begin{cases} \alpha = \dfrac{a}{\sqrt{a^2-1}}\cos(S-\varphi)\pm i\left[1-\dfrac{a^2}{a^2-1}\cos^2(S-\varphi)\right]^{1/2} & (E\lesssim V_B) \qquad (58a) \\ \alpha = a\cos(\mathrm{Re}S-\varphi)\pm i\left[1-a^2\cos^2(\mathrm{Re}S-\varphi)\right]^{1/2} & (E>V_B) \qquad (58b) \end{cases}$$

The condition that we have a stationary state, i.e. $|\alpha| = 1$ in eq. (54), implies that

$$1 \geq \begin{cases} \dfrac{a^2}{a^2-1}\cos^2(S-\varphi) & E\lesssim V_B \qquad (59a) \\ a^2\cos^2(\mathrm{Re}S-\varphi) & E>V_B \qquad (59b) \end{cases}$$

For $E \ll V_B$, $a^2 = (1+e^{-2\pi\varepsilon})$ $(\varepsilon \gg 0)$. Eq. (59a) then becomes, $\cos^2(S-\varphi) \lesssim e^{-2\pi\varepsilon}$ or

$$(n+\tfrac{1}{2})\pi - e^{-\pi\varepsilon} \lesssim S-\varphi \lesssim (n+\tfrac{1}{2})\pi + e^{-\pi\varepsilon} \qquad (60)$$

Since φ is small [1] and ε is large and positive, Eq. (60) is equivalent to the Bohr-Sommerfeld quantization rule and agree with the result of Ref. [13], where a linear mapping function is assumed for each turning point.

For $E >> V_B$, $a^2 = (1+e^{2\pi\varepsilon})$ ($\varepsilon<<0$). Eq.(59b) then becomes

$$\cos^2(\mathrm{ReS}-\varphi) \lesssim 1 - e^{2\pi\varepsilon} \qquad (\varepsilon << 0)$$

This condition is always satisfied, i.e. the electron is in the continuum.

At energies near the top of the potential barrier, the stationary state condition can be written as

$$(1 + e^{2\pi\varepsilon}) \cos^2(\mathrm{ReS}-\varphi) \leq 1 \tag{61}$$

where $\varepsilon > 0$ for $E \leq V_B$ and $\varepsilon < 0$ for $E > V_B$. A parabolic barrier implies that ε can be approximated by

$$\varepsilon = (V_B - E)/\hbar\omega_B \tag{62}$$

with

$$\hbar\omega_B = \sqrt{\frac{\hbar^2 |V''(r_B)|}{\mu}}$$

for energy near the barrier. r_B is the barrier position. Let us assume that the modified Bohr-Sommerfeld quantization rule is satisfied at E_0, i.e.

$$\mathrm{ReS}(E_0) - \varphi = (n + \tfrac{1}{2})\pi \tag{63}$$

Using a perturbation expansion, we can estimate then the band width Γ. Expanding ReS(E) around E_0 up to the first order, we have

$$\mathrm{ReS}(E) = \mathrm{ReS}(E_0) + \omega_0\tau \cdot \frac{(E-E_0)}{\hbar\omega_0} \tag{64}$$

where τ is the transit time through the potential well and $\hbar\omega_0$ is the level spacing, i.e. $\omega_0\tau = \pi$. Similarly ε can be written as

$$\varepsilon = \varepsilon_0 - \frac{E - E_0}{\hbar\omega_B} \qquad (65)$$

Then Eq.(61) gives,

$$[1 + e^{2\pi\varepsilon_0}(1 - \frac{\Gamma}{2\hbar\omega_B})](\sin^2 [(\frac{\Gamma}{2\hbar\omega_0}).\omega_0\tau]) \approx 1 \qquad (66)$$

Assuming that $\frac{\Gamma}{2\hbar\omega_B} << 1$, we have

$$\Gamma = \hbar\omega_0 . \frac{2}{\pi} (\sin^{-1}\sqrt{\frac{1}{1+e^{2\pi\varepsilon_0}}}) \qquad (67)$$

Here we used the fact that φ is small and is a slowly varying function of E (see I).

V. CONCLUSION

The wave propagation matrix method has been introduced to reformulate the semiclassical theory of multi-turning point problems. The wave propagation matrix is given as products of phase shift matrices and barrier transformation matrices. The wave function in any region of the real axis can easily be written down via the wave propagation matrix. This method is flexible and reliable in dealing with complicated problems. We worked out the barrier transformation matrices for the potential barrier which can be mapped onto a quadratic or a linear comparison functions. These barrier transformation matrices are useful in many physical problems.

This method was applied to study the characteristic properties of surface transparent potentials [3] in heavy ion scattering. The internal waves are reflected by the surface of the imaginary potential and by the most inner barrier. The interference of these two internal waves gives rise to oscillation in the amplitude of the total internal wave S matrix. Correspondingly, the phase shift of the total internal wave S matrix resembles that of a deep real potential. We found that the semiclassical theory of multiturning point problem is very powerful especially in studying the internal region of the optical potentials in light heavy ion scatterings. Another very informative phenomena in heavy

ion reactions are inelastic scattering and transfer reactions. For instance the cross section of the inelastic scattering of α particle on ^{40}Ca at backward angles shows close correlation to the elastic scattering cross section [14]. This implies that the internal region plays an important role also in the inelastic scattering. It is highly desirable to extend the wave propagation matrix method to describe the inelastic scattering and the transfer reactions.

ACKNOWLEDGEMENTS

The authors are grateful for the hospitality of the Division de Physique Théorique, Institut de Physique Nucléaire, Orsay and are pleased to acknowledge the financial support of the C.N.R.S.. We are indebted to Drs. D.M. Brink and C. Marty for their many valuable discussions and encouragements. We thank Dr. R. Behrman for careful reading of the manuscript. One of us (N.T.) thanks also a financial aid from the Iwanami Fujukai Foundation.

Appendix : Correlation between the poles of the optical potential and the turning points.

An optical potential is often represented by a function which contains poles. The Woods-Saxon form is one of the most common examples. In such cases, the position of the poles defines the surface region where the waves are mainly reflected. In semiclassical theory, reflection takes place at the turning point. Thus one may expect a close correlation between the poles of the optical potential and the turning points. One interesting question arises when the pole positions differ in the real and in the imaginary potentials, i.e. when they have different form factors. We have three turning points in the scattering from a real central potential. The question is:do we get more than three important turning points by switching on the imaginary part of the potential ? In other words, do we have additional processes of the reflection of waves by the surface of the imaginary potential ? We had two different examples, one in III.1 of this paper and another in III.4 of I. In the latter we had still only three important turning points. Whereas in the former we had additional two important turning points in the vicinity of the poles of the imaginary potential. In this Appendix, we clarify the difference between these two cases. Let us denote the leading poles of the real and the imaginary potentials by z_R and z_I. Near the poles, the turning point may be approximated by

$$\tilde{V}_0 \frac{1}{Z-Z_R} + i \tilde{W}_0 \frac{1}{Z-Z_I} = E \qquad (A.1)$$

with

$$\tilde{V}_0 = - V_0.a \quad \text{and} \quad \tilde{W}_0 = - W_0.a_W \quad , \qquad (A.2)$$

where (V_0,W_0) and (a,a_W) are the strength and the diffuseness parameters of the (real, imaginary) potentials respectively.

If $Z_R = Z_I = Z_0$, then

$$Z = Z_0 + \frac{1}{E} (\tilde{V}_0+i\tilde{W}_0) \quad . \qquad (A.3)$$

Eqs.(A.2) and (A.3) imply that there exists a turning point in the vicinity of the pole of the potential provided that the energy is very high or that the interaction is fairly weak [9].

When $Z_R \neq Z_I$, we study the solutions Z_1 and Z_2 of Eq.(A.1) in two different limits.

(a) The first is the case, when

$$|\frac{1}{E}(\tilde{V}_0+i\tilde{W}_0)| >> |\xi| \quad , \qquad (A.4)$$

where

$$\xi = Z_R - Z_I \quad .$$

The α-^{40}Ca scattering, studied in III.4 of I is an example. In this case,

$$Z_1 \simeq \frac{Z_R+Z_I}{2} + \frac{1}{E}(\tilde{V}_0+i\tilde{W}_0) + \frac{\xi}{2}\left\{\frac{\tilde{V}_0-i\tilde{W}_0}{\tilde{V}_0+i\tilde{W}_0}\right\} + \ldots \qquad (A.5a)$$

and

$$z_2 \sim \frac{Z_R+Z_I}{2} - \frac{\xi}{2} \frac{\tilde{V}_0 - i\tilde{W}_0}{\tilde{V}_0 + i\tilde{W}_0} + \ldots \qquad \text{(A.5b)}$$

We see that only one of the turning points z_2 is close to the pole of the potential. The other turning point is pushed away from the real axis and becomes unimportant.

(b) The second is the case, when

$$|\xi| >> \left| \frac{1}{E}(\tilde{V}_0 + i\tilde{W}_0) \right| . \qquad \text{(A.6)}$$

The $^{16}O-^{16}O$ scattering, studied in III.1 of this paper, is an example. In this case

$$z_1 \sim Z_R + \frac{1}{E}\tilde{V}_0 \qquad \text{(A.7a)}$$

and

$$z_2 \sim Z_I + i\frac{1}{E}\tilde{W}_0 . \qquad \text{(A.7b)}$$

Thus one can expect an additional turning point in the vicinity of the pole of the imaginary potential. This is what we have seen in Figs.2 and 5.

References

[1] K.W. Ford and J.A. Wheeler, Ann. Phys. (N.Y.) 7 (1959), 259 and 287 ;
W.H. Miller, J. Chem. Phys. 48 (1968), 1651 ;
Adv. Chem. Phys. 25 (1974), 69 ; Adv. Chem. Phys. 30 (1975), 77 ;
M.V. Berry and K.E. Mount, Rep. Prog. Phys. 35 (1972), 315 ;
N.L. Conner, Molecular Physics, 15 (1968), 621 ; 23 (1972), 717 ; 31 (1976), 1181.

[2] S.Y. Lee, N. Takigawa and C. Marty, "A semiclassical study of optical potentials - potential resonances", preprint Orsay IPNO/TH 77-19.

[3] A. Gobbi, R. Wieland, L. Chua, D. Shapira and D.A. Bromley, Phys. Rev. C7 (1973), 30.

[4] N.L. Connor, Molecular Phys. 25 (1973), 1469.

[5] D.M. Brink and N. Takigawa, Nucl. Phys. A279 (1977), 159.

[6] S.C. Miller and R.H.J. Good, Phys. Rev. 91 (1953), 174.

[7] M. Abramowitz and I.A. Stegun, "Handbook of Mathematical Functions", (Dover 1972).

[8] E.T. Whittaker and J.N. Watson, "A course of Modern Analysis", (C.U.P. 1963), p. 347.

[9] A. Zwaan, Intensitäten im Ca-Funkenspektrum. Arch. Néerlandaises des Sciences Exactes, 12 (1929) 1-76; R.B. Dingle, "Asymptotic Expansions : Their Derivation and Interpretation", Academic Press, London and New York (1973).

[10] J. Knoll and R. Schaeffer, Ann. of Phys. (N.Y.) 97 (1976), 307.

[11] L. Landau and E. Lifshitz, "Quantum Mechanics", Chap.7 MIR(URSS), 1967.

[12] V.L. Pokrovskii and I.M. Khalatnikov, Sov. Phys. JETP 13 (1961), 1207.

[13] D. ter Haar, "Selected Problems in Quantum Mechanics", (1964), Infosearch Ltd, London.

[14] R. Ceuleneer, F. Michel and R. Vanderporten, private communication.

FIGURE CAPTIONS

Fig.1 A typical potential of a double humped barrier is plotted as a function of r. Here r_4, r_3, r_3, r_2 and r_1 are the turning points for a particle with incident energy E.

Fig.2 The turning points of the surface transparent potential of $^{16}O - ^{16}O$ scattering are plotted. The potential parameters are listed in the brackets as (r_0, V_0, a_0) and (r_W, W_0, a_W). The number beside the turning point indicates the angular momentum value. The xV and xW indicate the pole positions of the real and the imaginary potentials respectively. The dashed curves show the turning points for the real potential only.

Fig.3 The real part of the semiclassical internal wave S matrix (thin solid line) is compared with that given by the quantum mechanical calculation (thick solid line). At large ℓ, η_I^Q goes to zero slowly. This is because η^B does not converge fast enough for large ℓ [5] . The dashed line indicates a possible modification.

Fig.4 The imaginary part of the semiclassical internal wave S matrix (thin solid line) is compared with that given by the quantum mechanical calculation (thick solid line). See Fig.3 for the dashed line.

Fig.5 The amplitudes of the internal wave S matrices are compared for the surface transparent potential. η_I^3 and η_I^4 are the semiclassical S matrices of the internal waves reflected from the turning points r_3 and r_4 respectively. See Fig.3 for the dashed lines.

Fig.6 The same diagram as in Fig.2, but for the case of the potential studied by Gobbi et al. [2].

Fig.7 The same diagram as in Fig.5 but for the case of the potential studied by Gobbi et al. [2].

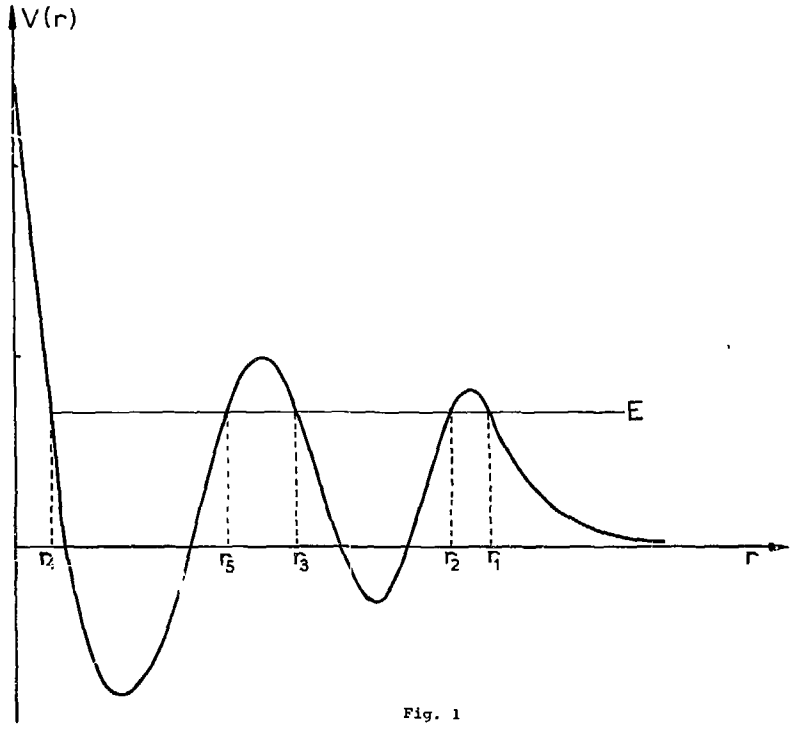

Fig. 1

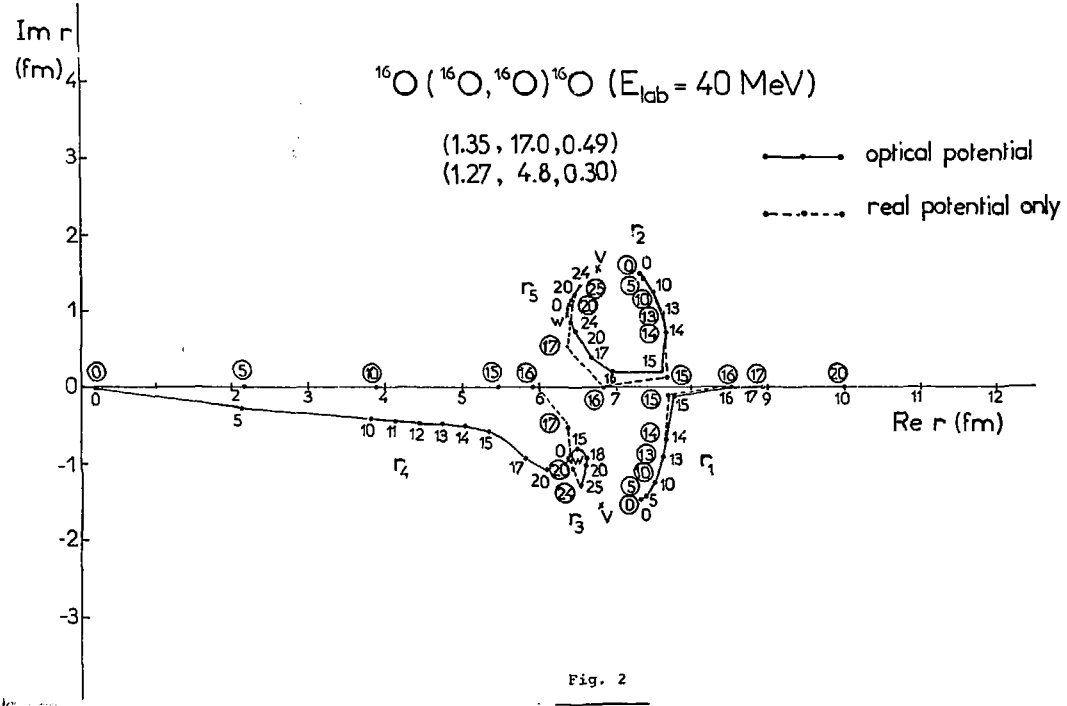
Im r
(fm)
$^{16}O(^{16}O,^{16}O)^{16}O$ (E_{lab} = 40 MeV)
(1.35, 17.0, 0.49)
(1.27, 4.8, 0.30)
optical potential
real potential only
Re r (fm)
r_1
r_2
r_3
r_4
r_5

Fig. 2

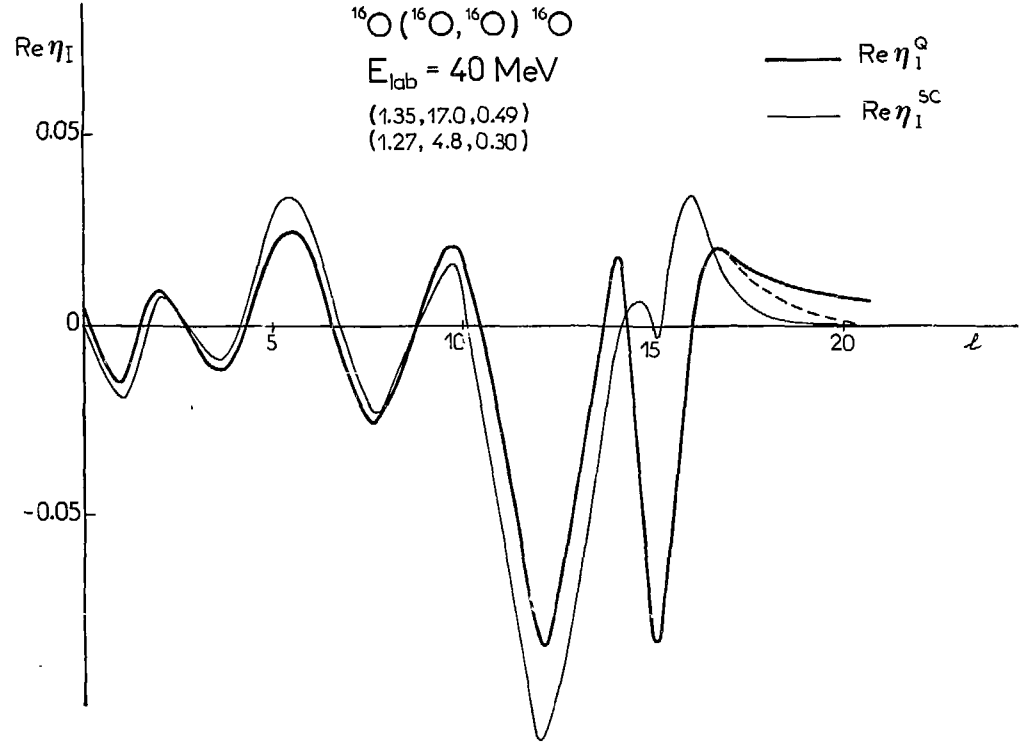
$^{16}O(^{16}O,^{16}O)\,^{16}O$
E_{lab} = 40 MeV
(1.35, 17.0, 0.49)
(1.27, 4.8, 0.30)
$Re\,\eta_I$
$Re\,\eta_l^Q$
$Re\,\eta_l^{SC}$
0.05
0
-0.05
5
10
15
20
l

Fig. 3

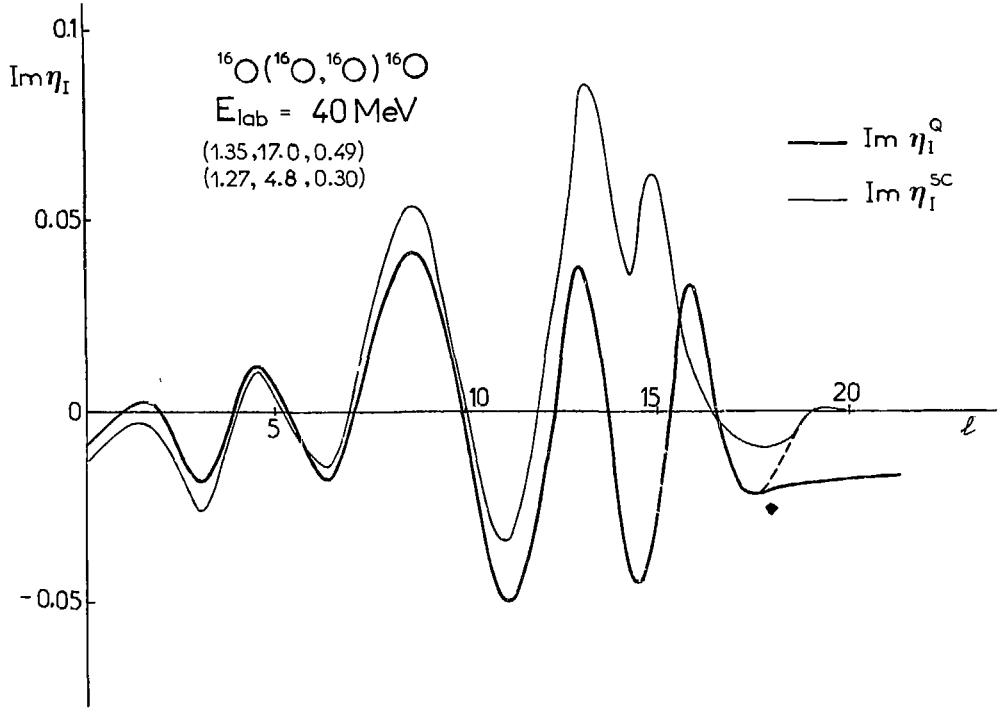
0.1
Im η_I
$^{16}O(^{16}O,^{16}O)^{16}O$
E_{lab} = 40 MeV
(1.35, 17.0, 0.49)
(1.27, 4.8, 0.30)
Im η_I^Q
Im η_I^{SC}
0.05
0
-0.05
5
10
15
20
ℓ

Fig. 4

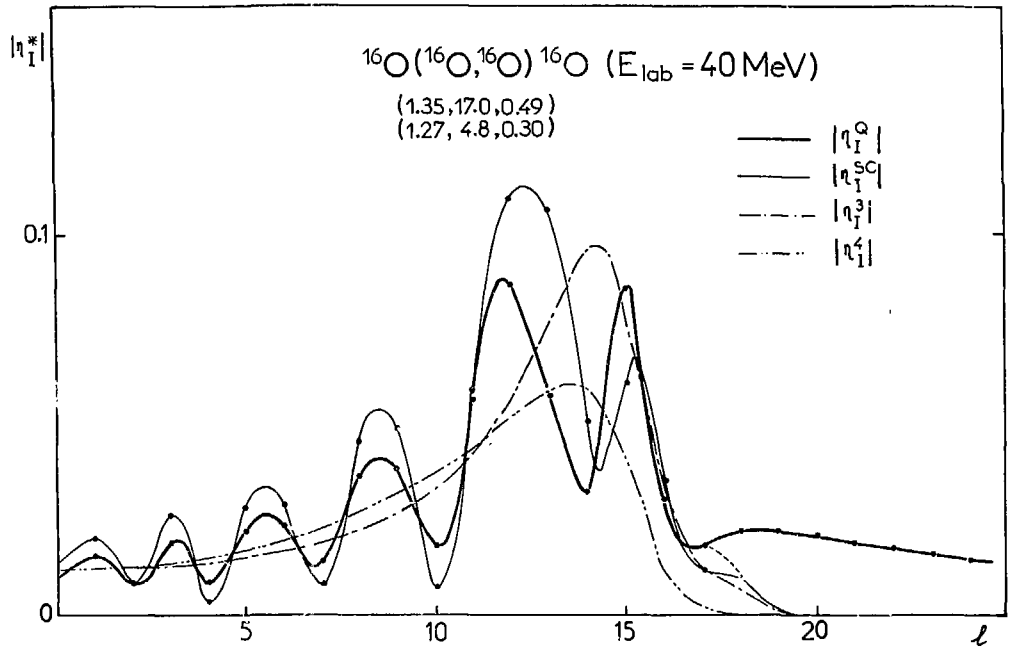
$|\eta_I^*|$
$^{16}O(^{16}O,^{16}O)^{16}O$ (E_{lab} = 40 MeV)
(1.35, 17.0, 0.49)
(1.27, 4.8, 0.30)
$|\eta_I^Q|$
$|\eta_I^{SC}|$
$|\eta_I^3|$
$|\eta_I^4|$
0.1
0
5
10
15
20
ℓ

Fig. 5

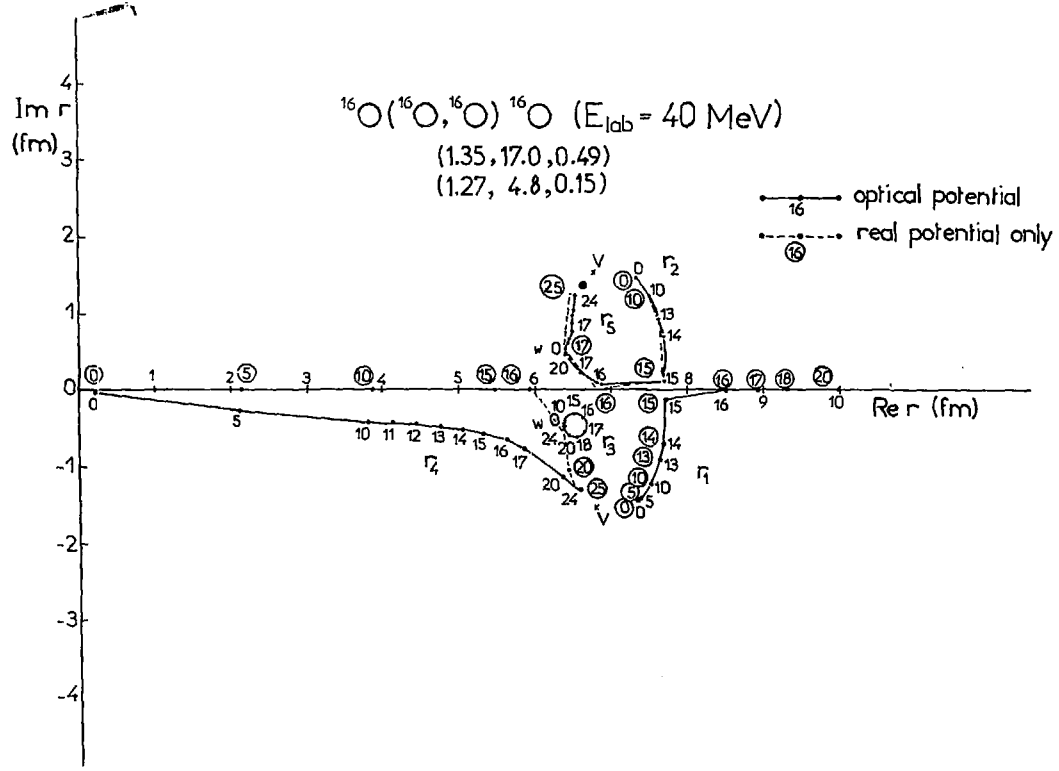
$^{16}O(^{16}O,^{16}O)\,^{16}O$ (E_{lab} = 40 MeV)
(1.35, 17.0, 0.49)
(1.27, 4.8, 0.15)
optical potential
real potential only
Im r (fm)
Re r (fm)
V
W
r_1
r_2
r_3
r_4
r_5

Fig. 6

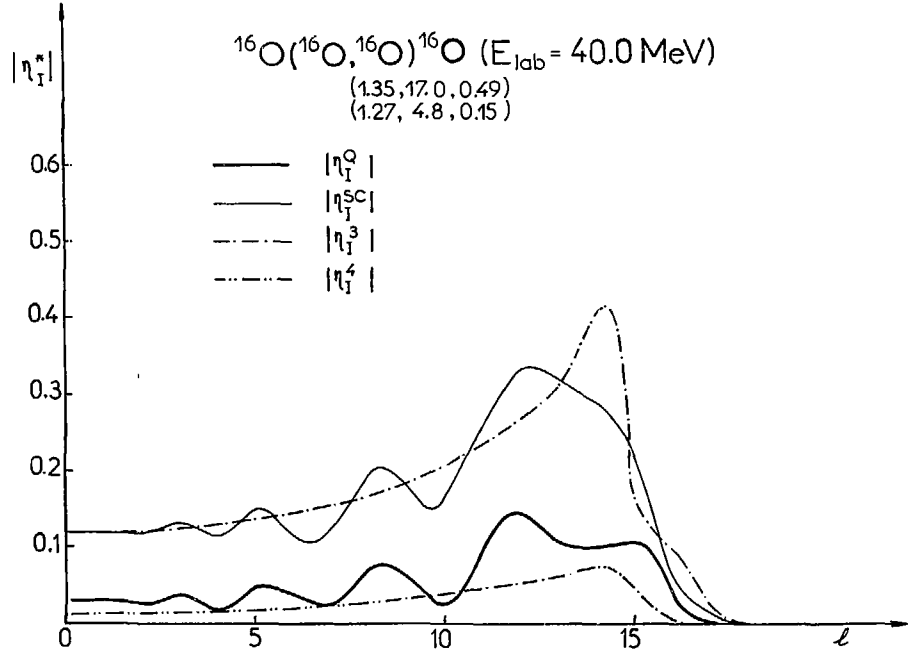
$^{16}O(^{16}O,^{16}O)^{16}O$ (E_{lab} = 40.0 MeV)
(1.35, 17.0, 0.49)
(1.27, 4.8, 0.15)
$|\eta_I^N|$
$|\eta_I^Q|$
$|\eta_I^{SC}|$
$|\eta_I^3|$
$|\eta_I^4|$
0.6
0.5
0.4
0.3
0.2
0.1
0
5
10
15
ℓ

Fig. 7